Unique vortex and stripe domain structures in $PbTiO_3$ epitaxial nanodots

L. Hong and A. K. Soh*

Department of Mechanical Engineering, The University of Hong Kong, Hong Kong, China

Abstract

The domain structures of $PbTiO_3$ epitaxial nanodots under the influences of depolarization fields and mismatch strains have been studied using three dimensional phase field simulations. The single-vortex structure and mixed domain configuration, which consisted of zigzag stripe domain and closure dipole flux near the interfaces, were found to be effective in annihilating the depolarization fields in the isotropically tensile and compressive ferroelectric nanodots, respectively. These domain structures were produced by the combined effect of electrostatic and mismatch elastic energies. The width of stripe domain was found to be related to the volume percentage of polarization dipoles along the *z*-axis, which varied remarkably with the change of compressive mismatch strain. In the case of nanodots under anisotropic mismatch strains, double-vortex domain patterns and stripe domains with nearly straight domain walls were formed. Moreover, the domain structures with electrostatic energy neglected were also studied.

* To whom all correspondence should be addressed (aksoh@hkucc.hku.hk)
Tel: +852-28598061
Fax: +852-28585415

Keywords: Phase-field model; Ferroelectric; Vortex; Epitaxial nanodots; Mismatch strains

1. Introduction

Ever since the discovery of vortex domain structures in ferroelectric nanodots and nanowires (Naumov et al., 2004), tremendous efforts have been made by researchers to study their intrinsic formation mechanisms. Recently, some unique stripe domains were shown to exist in ferroelectric epitaxial nanostructures (Naumov and Bratkovsky, 2008). The emergences of these special domain patterns provide both challenges and aspirations for the present technology. On one hand, the persistent requirement to decrease the size of a ferroelectric functional unit while keeping the dipole states detectable is the driving force that leads to the reduction of the nanodot density of $Pb(Zr_{0.20}Ti_{0.80})O_3$ (PZT) nanocapacitor arrays to near Tb $inch^{-2}$ (Lee et al., 2008). On the other hand, novel techniques used to readout the ferroelectric states, such as non-destructive approaches (Garcia et al., 2009) and high-resolution piezoresponse force microscopy (Ivry et al., 2009), are readily available. Since the formation and manipulation of the special domain patterns in ferroelectric nanostructures have significant influences on the development of nanoferroelectric technology, it is vital to achieve a better understanding of such influences, especially in epitaxial nanodots.

It is a known fact that in ferroelectric thin films the mismatch strains originating from lattice misfits between the nanostructure and substrate have significant influences

on the ferroelectric domain phases (Janolin, 2009; Li and Chen, 2006). Moreover, compared with a continuous thin film, a nanodot structure is highly confined in three dimensions, which leads to significant differences in elastic stress (Zhang et al., 2008) and depolarization distributions. Individual ferroelectric nanodots or nanoparticles have been found to possess special vortex domain structures under open-circuit condition (Naumov et al., 2004; Wang et al., 2008). Thus, it is interesting to study the domain structures of ferroelectric nanodots epitaxially grown on substrates under the combined effects of depolarization field and mismatch strains.

In the present study, a three dimensional phase field model, which is similar to those developed by Slutsker et al. (2008) and Zhang et al. (2008), is devised to investigate the effects of mismatch strains and depolarization fields on the $PbTiO_3$ (PTO) epitaxial nanodots under open-circuit condition. The size of this computational model is 64×64×48 discrete grids, in which the ferroelectric nanodot of size 32×32×16 is positioned at the center epitaxially on the substrate of thickness 16 discrete grids, and embedded in the gas medium, as shown in Fig. 1. Compared with other phase field models developed for the study of nanoferroelectric domain structures, the present model can easily illustrate distinguishable domain patterns, i.e. single or double-vortex and straight or zigzag stripe domain structures, providing a delicate solution to probe these special domain patterns individually. Besides, this model can be easily modified to include the mismatch strains at the vertical interfaces if the gas medium is replaced with some dielectric material which is epitaxially connected to the ferroelectric nanodot.

2. Phase field model

The time-dependent Ginzburg-Landau (TDGL) equation is employed to govern the evolution of the time and spatial dependent spontaneous polarizations, i.e. $\frac{\partial P_i(\mathbf{r},t)}{\partial t} = -L\frac{\delta F}{\delta P_i(\mathbf{r},t)}$, where $\mathbf{r}$ denotes spatial vector; P_i represents spontaneous polarization, and $i = 1,2,3$ denotes x, y and z, respectively. In addition, t and L are the time and kinetic coefficient, respectively. The total energy (F) of the system is composed of bulk free energy (F_L), gradient energy (F_G), elastic energy (F_{ela}) and electrostatic energy ($F_{electro}$), i.e., $F = F_L + F_G + F_{ela} + F_{electro}$. The expressions of these energy terms can be found in Hong et al. (2009) and Li et al. (2002). A six-order polynomial is used as Landau-Devonshire potential for the bulk free energy as follows:

$$F_L = \int_V \begin{Bmatrix} \alpha_1(P_1^2+P_2^2+P_3^2)+\alpha_{11}(P_1^4+P_2^4+P_3^4)+\alpha_{12}(P_1^2P_2^2+P_2^2P_3^2+P_3^2P_1^2) \\ +\alpha_{111}(P_1^6+P_2^6+P_3^6)+\alpha_{112}[P_1^4(P_2^2+P_3^2)+P_2^4(P_1^2+P_3^2)+P_3^4(P_1^2+P_2^2)] \\ +\alpha_{123}(P_1^2P_2^2P_3^2) \end{Bmatrix} dV, \quad (1)$$

where α_1 is the temperature dependent dielectric stiffness constant; and other coefficients are temperature independent higher order dielectric stiffness constants. The gradient energy $F_G = \frac{1}{2}\int_V \beta_{ijkl}P_{i,j}P_{k,l}dV$ represents the domain wall energy in the ferroelectric nanodot, where β_{ijkl} are the gradient energy coefficients; and the commas in the subscripts denote spatial differentiation. The elastic energy is expressed as

$$F_{ela} = \frac{1}{2}\int_V c_{ijkl}(\mathbf{r})(\varepsilon_{ij}(\mathbf{r})-\varepsilon_{ij}^0(\mathbf{r}))(\varepsilon_{kl}(\mathbf{r})-\varepsilon_{kl}^0(\mathbf{r}))dV, \quad (2)$$

where $c_{ijkl}(\mathbf{r})$ and $\varepsilon_{ij}(\mathbf{r})$ are the elastic stiffness tensors and total strains, respectively. The stress-free strains $\varepsilon_{ij}^{0}(\mathbf{r})$ consist of two parts: the spontaneous strains generated during ferroelectric phase transition from cubic to tetragonal, and the mismatch strains induced by different lattice parameters between the nanodot and substrate, i.e. $\varepsilon_{ij}^{0}(\mathbf{r}) = Q_{ijkl}(\mathbf{r})P_k(\mathbf{r})P_l(\mathbf{r}) + \varepsilon_{ij}^{mis}(\mathbf{r})$, in which $Q_{ijkl}(\mathbf{r})$ are the electrostrictive coefficients. The mismatch strains are defined with respect to the substrate, i.e. $\varepsilon_{ij}^{mis}(\mathbf{r}) = (a_{PTO} - a_{sub})/a_{sub}$, where a_{PTO} and a_{sub} are the lattice parameters of PTO and substrate, respectively. In this case, only the in-plane components are considered, i.e. $\varepsilon_{zz}^{mis} = \varepsilon_{xy}^{mis} = \varepsilon_{yz}^{mis} = \varepsilon_{xz}^{mis} = 0$ and $\varepsilon_{xx}^{mis} = \varepsilon_{yy}^{mis} = \mathrm{u_m}$ (for the case of isotropic mismatch) or $(\varepsilon_{xx}^{mis} = \mathrm{u_m^{xx}}) \neq (\varepsilon_{yy}^{mis} = \mathrm{u_m^{yy}})$ (for the case of anisotropic mismatch). As the present model is elastic but inhomogeneous, an iterative method (Hu and Chen, 2001) is used to obtain the elastic solution. Besides, all the stress-free boundary conditions applied onto the surfaces of the PTO nanodot can be automatically satisfied since the elastic constants of gas are zero. For simplicity, the elastic moduli of the substrate are assumed to be the same as those of the ferroelectric part even though the case of different elastic moduli can also be investigated using the same approach. The electrostatic energy is induced by the inhomogeneous polarizations, i.e. $F_{electro} = -\frac{1}{2}\int_v E_i(\varepsilon_0\kappa_{ij}E_j + P_i)dV$ where E_i, ε_0 and κ_{ij} represent the electrostatic field, the dielectric constant of vacuum and the relative dielectric constant, respectively. In the present study, κ_{ij} are considered as isotropic and homogeneous constants for the whole model. The Maxwell's equation is employed to determine the electrostatic potential using the finite difference method under the open-

circuit boundary condition. Sufficient simulation steps are carried out to obtain stable and convergent results.

All the parameters used in the present simulation are listed as follows. The coefficients of the bulk free and elastic energies (in SI units and the temperature is in ^{o}C) are: $\alpha_1 = 3.8\times(T-479)\times10^5$, $\alpha_{11} = -7.3\times10^7$, $\alpha_{12} = 7.5\times10^8$, $\alpha_{111} = 2.6\times10^8$, $\alpha_{112} = 6.1\times10^8$, $\alpha_{123} = -3.7\times10^9$, $Q_{11} = 0.089$, $Q_{12} = -0.026$, $Q_{44} = 0.03375$, $c_{11} = 1.75\times10^{11}$, $c_{12} = 7.94\times10^{10}$, $c_{44} = 1.11\times10^{11}$, $T = 27$, which are obtained from Li et al. (2002a, 2002b). The spontaneous polarization, and relative dielectric constant and the reference values of the gradient energy coefficient are $P_0 = 0.757$ Cm^{-2} , $\kappa_{11} = \kappa_{22} = \kappa_{33} = 66$ and $\beta_{110} = 1.73\times10^{-10}$ C^{-2}m^{4}N , respectively (Li et al., 2002a). The gradient energy coefficients are assumed as $\beta_{11}/\beta_{110} = 2$, $\beta_{12}/\beta_{110} = 0$, $\beta_{44}/\beta_{110} = 1$ and $\beta_{44}^{'}/\beta_{110} = 1$. The grid spacing along the three axes are the same, i.e., $\Delta x = \Delta y = \Delta z = l_0$, where $l_0 = \sqrt{\beta_{110}/|\alpha_1|} = 1$ nm.

3. Results and discussion

3.1. Isotropic mismatch strains

The single-vortex structure in which the polarization dipoles aligning with the confined boundaries of the PTO nanodot is stabilized when the isotropic mismatch strains

are not larger than zero ($u_m \le 0$), as shown in Fig. 2a, due to the strain-dipole coupling (Pertsev et al., 1998) and the annihilation of the depolarization fields. If the electrostatic energy is not considered, the domain structures formed will be very different, which will be shown later. Fig. 2b-2d present the domain structures of ferroelectric nanodot under different compressive mismatch strains. When u_m is equal to 0.01, the original vortex structure lying on the (001) plane disappear, and instead out-of-plane 180^o stripe domains are produced alternating between the [100] and [010] direction. The in-plane polarizations, which constitute 40% of the total dipoles as shown in Fig. 2c, symmetrically lie on the upper and bottom interfaces to seal part of the dipole flux. Such domain configuration can be taken as a combination of Landau-Lifshitz closure domain structure (Landau and Lifshitz, 1935) and Kittel vertical stripe pattern (Kittel, 1946), whose existence in ferroelectric thin films due to poor screening of depolarization fields has been illustrated (Prosandeev and Bellaiche, 2007). This special domain configuration arises from the competition between the compressive mismatch elastic energy and the electrostatic energy. This is because the compressive mismatch strains are well known for preference of *c*-domains along the *z*-axis (Pertsev et al., 1998), while the stripe domains with in-plane polarizations that form dipole flux are effective in suppressing the depolarization field inside the nanodot. Fig. 2d displays the predominating stripe domains which constitute nearly 90% of the whole ferroelectric body when the isotropic mismatch strain is increased to 0.05; meanwhile some in-plane polarizations exist at the upper and lower interfaces to connect the antiparallel polarization dipoles along the *z*-axis. The width of the stripe domain on the (100) plane in Fig. 2d is larger than that in Fig. 2c by a ratio of 4/3, which has also been found in both experimental and numerical studies on

180^o stripe domains in ferroelectric thin films (Prosandeev and Bellaiche, 2007; Streiffer et al., 2002). By combining with the results provided in Prosandeev and Bellaiche (2007), the width of the stripe domain in ferroelectric nanostructures can be correlated with the volume percentage of stripe domains which are remarkably affected by compressive mismatch strains and dead layer thicknesses (Prosandeev and Bellaiche, 2007). Note that although similar variation of domain patterns with mismatch strains has been identified in lower dimensional nanoferroelectrics using first-principle calculations (Ponomareva et al., 2005), the special mixed domain consisting of zigzag stripe domain and closure dipole flux was not mentioned in the existing works. In addition, to the best of our knowledge, to-date, the mentioned domain configuration has never been studied by the phase field method.

Fig. 3 presents the variation of toroidal moment G_z per unit cell, whose definition is the same as that provided in Naumov et al. (2004), and percentage of P_z with isotropic mismatch strain, where P_z percentage is the volume of polarizations along the *z*-axis of the ferroelectric nanodot. In the case where the nanodot is subjected to tensile mismatch strains, stable single-vortex structure with significant G_z value and null P_z is always obtained. When the compressive mismatch strain is larger than 0.003 the original vortex structure disappears, instead zigzag and not straight stripes (refer to Fig. 2c and 2d) are formed, which is similar to the domain structures that exist in $BaTiO_3$ nanoparticles (Naumov and Bratkovsky, 2008), except that in the present PTO nanodot in-plane polarizations apparently exist at the top and bottom interfaces to form closure dipole flux. In addition, the intermediate domain phase presented in Fig. 2b, which is remarkably

different from the Skyrmion-like intermediate phase (Naumov and Bratkovsky, 2008), reveals that the transformation "vortex-to-stripe" starts from the formation of vertical domains on one lateral plane.

3.2. Anisotropic mismatch strains

Anisotropic mismatch strains were found to have significant effects on the dielectric constants (Lin et al., 2004) and the strain-temperature domain stability diagrams (Zembilgotov et al., 2005; Sheng et al., 2008a) of ferroelectric nanostructures compared to the isotropic ones. For the present PTO nanodot, under the influences of confined boundaries and depolarization fields, some unique vortex and stripe domain structures are produced by the anisotropic mismatch strains. An asymmetric double-vortex domain structure in which in-plane polarization dipoles along the *x*-direction are the majority, as shown in Fig. 4a, exist when the strains are set as $u_m^{xx} = -0.01$ and $u_m^{yy} = 0.0$. Obviously, it is due to the fact that both the tensile and zero mismatch strains prefer in-plane polarizations, meanwhile the majority of these dipoles rotate to the direction of larger tensile strain. This is the first discovery of such double-vortex domain pattern located on the growth plane of the ferroelectric nanodot. Fig. 4b presents another double-vortex domain pattern situated on the *yz*-plane because $u_m^{xx} = 0.01$ favors *c*-domain while $u_m^{yy} = 0.0$ prefers in-plane dipoles. In comparison with the isotropic case (refer to Fig. 2c), the decrease of the compressive mismatch strain along the *y*-axis from 0.01 to zero reduces the volume portion of the *c*-domain, and the labyrinthic domain walls become orderly (refer to Fig. 4b). By prescribing a positive u_m^{yy}

to the nanodot, the volume of in-plane polarization dipoles increases and single-vortex domain pattern is formed, as shown in Fig. 4c.

The domain structures under very high anisotropic mismatch strains can be significantly different from those under isotropic strains (refer to Fig. 2) or low anisotropic ones (refer to Fig. 4). Stripe domains become clear and prominent when compressive mismatch strains are applied along both the *x* and *y*-directions and at least one of the two strains is sufficiently large. Fig. 5a presents a domain structure in which the *a*- and *c*-domains coexist. However, for the case of $u_m^{xx} = 0.0$ and $u_m^{yy} = 0.05$, the domain structure is similar to that shown in Fig. 4b in which the double-vortex domain pattern is situated on the *xz*-plane (not shown here). With the increase of compressive strain in the *x*-direction, the *a*-domain portion decreases and stripe domains with nearly straight domain wall along the diagonal of *xy*-plane are formed (refer to Fig. 5b and 5c). For the case of $u_m^{xx} = 0.04$ and $u_m^{yy} = 0.05$, zigzag stripe domains with closure dipole flux on the upper and bottom surfaces, similar to that due to isotropic mismatch strain shown in Fig. 2d, is clearly formed. This result is in agreement with that obtained by first-principles calculations, which showed that a zigzag stripe pattern can be transformed to a normal stripe pattern when large anisotropic mismatch strains are prescribed (Naumov and Bratkovsky, 2008). The nearly straight stripe domain wall along diagonal direction and the zigzag stripe domain wall are compared in Fig. 6.

Compared with the case of ferroelectric thin film under short-circuit condition studied by Sheng et al. (2008a, 2008b) using the phase field method, the domain patterns

obtained in the present study show some similar correlation between the domain structures and mismatch strains, i.e. the preference of *a* and *c* domains when a ferroelectric nanostructure is subjected to applied tensile and compressive mismatch strains, respectively, and the remarkable differences of domain structures between the case of isotropic and anisotropic. However, since the existence of depolarization field due to the adoption of open-circuit condition significantly affects the domain patterns, the single-vortex and double-vortex patterns as well as the stripe domains with closure dipole flux are obviously different from the previously reported patterns.

3.3. Without electrostatic energy

The electrostatic energy is important for producing the above discussed irregular domain structures, all of which can effectively minimize the residual polarization charges on ferroelectric nanodot surfaces and, hence, annihilate the depolarization fields. However, in some cases the depolarization fields can be adequately compensated by interfacial free charges, e.g., by exposing a ferroelectric thin film to an ionic adsorbate (Fong et al., 2006), a monodomain may be stabilized. Therefore, there is a need to study the domain structures of PTO nanodot without accounting for the electrostatic energy, which are shown in Fig. 7. Both *c* and *a*-domains exist when the mismatch strain is zero (refer to Fig. 7a), and single *c*-domain with polarizations pointing in the same direction is induced by compressive mismatch strains (not shown here). The latter domain structure is the same as that of the corresponding thin film studied in Fong et al. (2006). The tensile mismatch strain $u_m = 0.01$ results in formation of periodical *a*-domains with 90^o domain

walls parallel to the (110) planes (refer to Fig. 7b). With the increase of tensile mismatch strains, the *a*-domains separated by 90^o domain walls become complex, however, there is no formation of in-plane vortex structure. Thus, it can be inferred that the tensile mismatch strains are prone to create in-plane polarization dipoles, while 90^o domain walls are produced for elastic relaxation.

4. Summary

In summary, a three dimensional phase field model has been devised to study several unique domain structures in PTO epitaxial nanodots. The depolarization fields as well as the isotropic/anisotropic mismatch strains show remarkable influences on the domain patterns. Single-vortex structures and mixed domain configurations, which consist of zigzag stripe domain patterns and closure dipole fluxes, are produced to suppress the depolarization fields in nanodots due to the combined effects of electrostatic and isotropic mismatch elastic energies. The width of the stripe domain is found to be related to the volume percentage of polarizations along the *z*-axis, which are significantly affected by compressive mismatch strains. The intermediate phase between the above two domain configurations is a combination of vortex structure and stripe domain. A unique double-vortex structure emerges as one prototype domain pattern under low anisotropic mismatch strains; while stripe domains with nearly straight domain wall along the in-plane diagonal are formed under very high anisotropic mismatch strains. Finally, obvious differences between the domain structures are observed if the electrostatic energy is not considered.

Acknowledgement

Support from the Research Grants Council of the Hong Kong Special Administrative Region, China (Project nos. HKU716508E and 716007E) is acknowledged. The authors gratefully acknowledge the support of the Computer Center of The University of Hong Kong.

Reference:

Fong, D.D., Kolpak, A.M., Eastman, J.A., Streiffer, S.K., Fuoss, P.H., Stephenson, G.B., Thompson, C., Kim, D.M., Choi, K.J., Eom, C.B., Grinberg, I., Rappe, A.M., 2006. Stabilization of monodomain polarization in ultrathin $PbTiO_3$ films. Phys. Rev. Lett. 96, 127601.

Garcia, V., Fusil, S., Bouzehouane, K., Enouz-Vedrenne, S., Mathur, N.D., Barthelemy, A., Bibes, M., 2009. Giant tunnel electroresistance for non-destructive readout of ferroelectric states. Nature 460, 81-84.

Hong, L., Soh, A.K., Liu, S.Y., Lu, L., 2009. Influence of size-dependent electrostatic energy on the ferroelectric nanodot domain structure by phase field method. J. Phys. D: Appl. Phys. 42, 122005.

Hu, S.Y., Chen, L.Q., 2001. A phase-field model for evolving microstructures with strong elastic inhomogeneity. Acta Mater. 49, 1879-1890.

Ivry, Y., Chu, D., Durkan, C., 2009. Nanometer resolution piezoresponse force microscopy to study deep submicron ferroelectric and ferroelastic domains. Appl. Phys. Lett. 94, 162903.

Janolin, P.E., 2009. Strain on ferroelectric thin films. J. Mater. Sci. 44, 5025-5048.

Kittel, C., 1946. Theory of the structure of ferromagnetic domains in films and small particles. Phys. Rev. 70, 965-971.

Landau, L., Lifshitz, E., 1935. On the theory of the dispersion of magnetic permeability in ferromagnetic bodies. Phys. Z. Sowjetunion 8, 153-169.

Lee, W., Han, H., Totnyk, A., Schubert, M.A., Senz, S., Alexe, M., Hesse, D., Baik, S., Gosele, U., 2008. Individually addressable epitaxial ferroelectric nanocapacitor arrays with near Tb $inch^{-2}$ density. Nat. Nanotechnol. 3, 402-407.

Li, Y.L., Hu, S.Y., Liu, Z.K., Chen, L.Q., 2002a. Effect of electrical boundary conditions on ferroelectric domain structures in thin films. Appl. Phys. Lett. 81, 427-429.

Li, Y.L., Hu, S.Y., Liu, Z.K., Chen, L.Q., 2002b. Effect of substrate constraint on the stability and evolution of ferroelectric domain structures in thin films. Acta Mater. 50, 395-411.

Li, Y.L., Chen, L.Q., 2006. Temperature-strain phase diagram for $BaTiO_3$ thin films. Appl. Phys. Lett. 88, 072905.

Lin, Y., Chen, X., Liu, S.W., Chen, C.L., Lee, J., Li, Y., Jia, Q.X., Bhalla, A., 2004. Anisotropic in-plane strains and dielectric properties in (Pb,Sr)TiO_3 thin films on $NdGaO_3$ substrates. Appl. Phys. Lett. 84, 577-579.

Naumov, I.I., Bellaiche, L., Fu, H., 2004. Unusual phase transitions in ferroelectric nanodisks and nanorods. Nature 432, 737-740.

Naumov, I.I, Bratkovsky, A., 2008. Unusual polarization patterns in flat epitaxial ferroelectric nanoparticles. Phys. Rev. Lett. 101, 107601.

Pertsev, N.A., Zembilgotov, A.G., Tagantsev, A.K., 1998. Effect of mechanical boundary conditions on phase diagrams of epitaxial ferroelectric thin films. Phys. Rev. Lett. 80, 1988-1991.

Ponomareva, I., Naumov, I.I., Bellaiche, L., 2005. Low-dimensional ferroelectrics under different electrical and mechanical boundary conditions: Atomistic simulations. Phys. Rev. B 72, 214118.

Prosandeev, S., Bellaiche, L., 2007. Asymmetric screening of the depolarizing field in a ferroelectric thin film. Phys. Rev. B 75, 172109.

Sheng, G., Zhang, J.X., Li, Y.L., Choudhury, S., Jia, Q.X., Liu, Z.K., Chen, L.Q., 2008a. Misfit strain–misfit strain diagram of epitaxial $BaTiO_3$ thin films: Thermodynamic calculations and phase-field simulations. Appl. Phys. Lett. 93, 232904.

Sheng, G., Zhang, J.X., Li, Y.L., Choudhury, S., Jia, Q.X., Liu, Z.K., Chen, L.Q., 2008b. Domain stability of $PbTiO_3$ thin films under anisotropic misfit strains: Phase-field simulations. J. Appl. Phys. 104, 054105.

Slutsker, J., Artemev, A., Roytburd, A., 2008. Phase-field modeling of domain structure of confined nanoferroelectrics. Phys. Rev. Lett. 100, 087602.

Streiffer, S.K., Eastman, J.A., Fong, D.D., Thompson, C., Munkholm, A., Murty, M.V.R., Auciello, O., Bai, G.R., Stephenson, G.B., 2002. Observation of nanoscale 180° stripe domains in ferroelectric $PbTiO_3$ Thin Films. Phys. Rev. Lett. 89, 067601.

Wang, J., Kamlah, M., Zhang, T.Y., Li, Y.L., Chen, L.Q., 2008. Size-dependent polarization distribution in ferroelectric nanostructures: Phase field simulations. Appl. Phys. Lett. 92, 162905.

Zembilgotov, A.G., Pertsev, N.A., Bo̎ttger, U., Waser, R., 2005. Effect of anisotropic in-plane strains on phase states and dielectric properties of epitaxial ferroelectric thin films. Appl. Phys. Lett. 86, 052903.

Zhang, J.X., Wu. R., Choudhury, S., Li, Y.L., Hu, S.Y., Chen, L.Q., 2008. Three-dimensional phase-field simulation of domain structures in ferroelectric islands. Appl. Phys. Lett. 92, 122906.

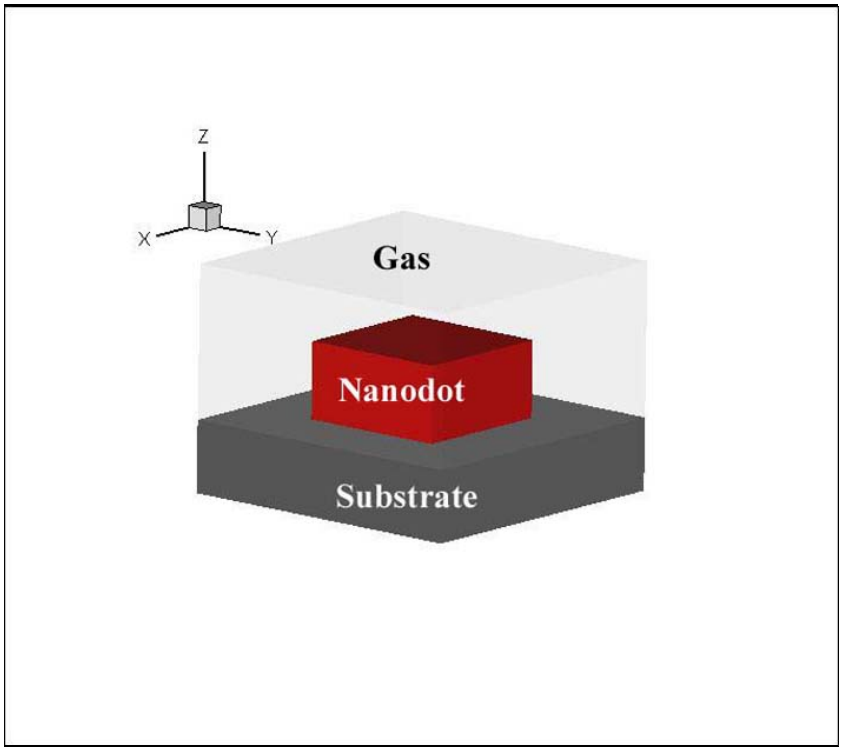

Fig.1

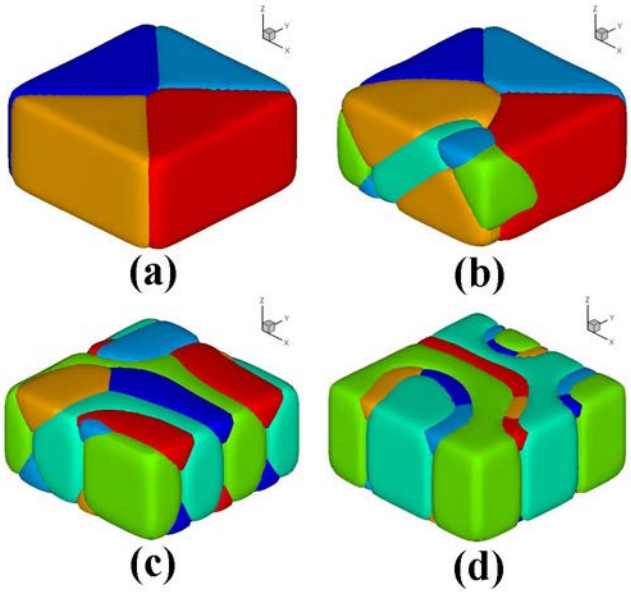

Fig. 2

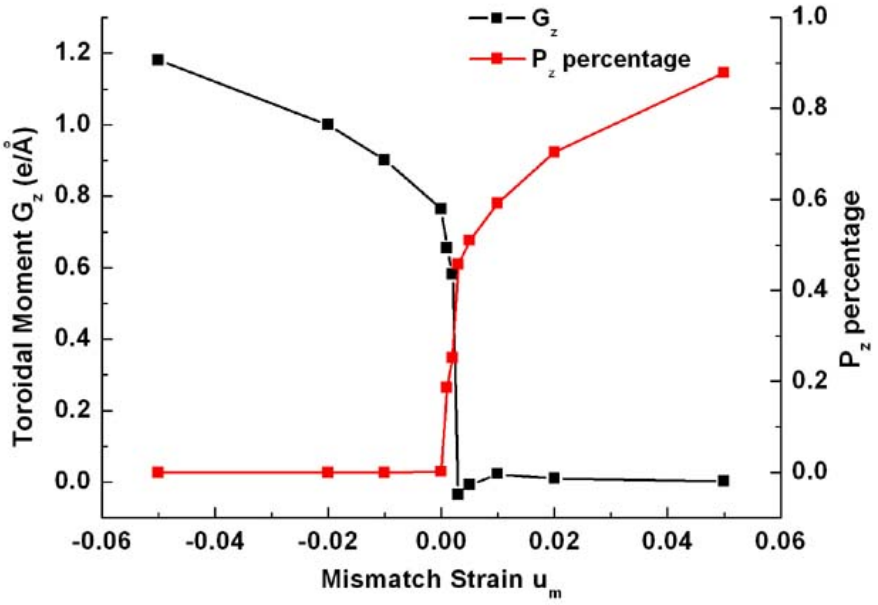
G_z
P_z percentage
Toroidal Moment G_z (e/Å)
P_z percentage
Mismatch Strain u_m
1.2
1.0
0.8
0.6
0.4
0.2
0.0
1.0
0.8
0.6
0.4
0.2
0.0
-0.06
-0.04
-0.02
0.00
0.02
0.04
0.06

Fig. 3

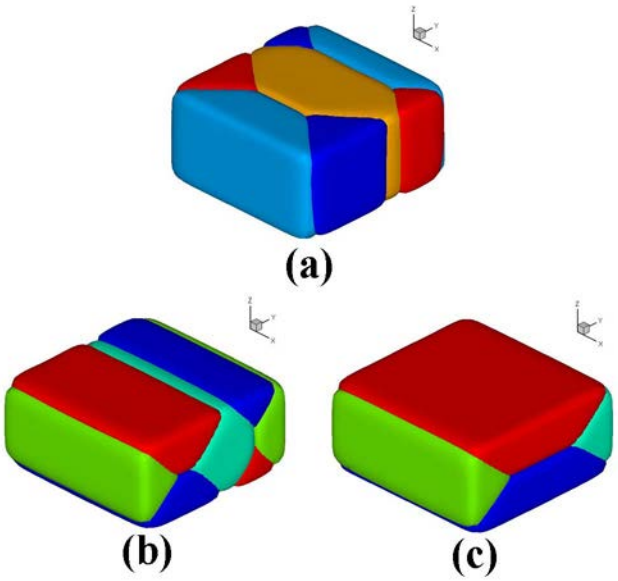
(a)
(b)
(c)

Fig. 4

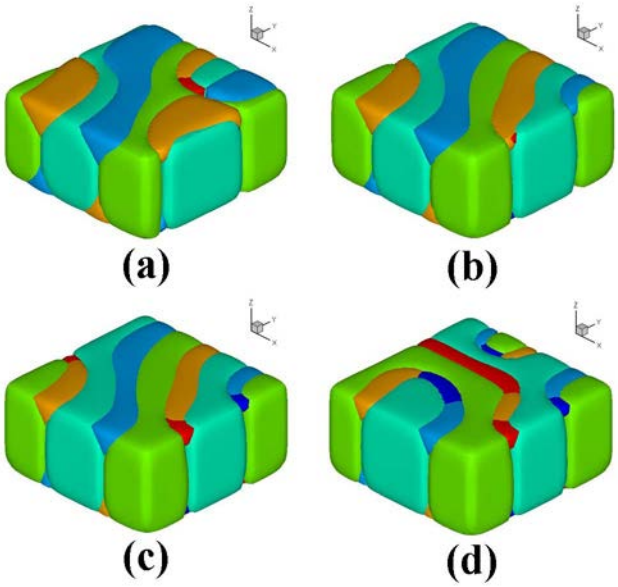

Fig. 5

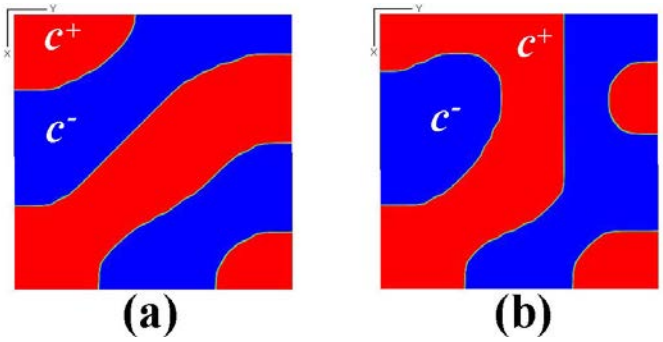

Fig. 6

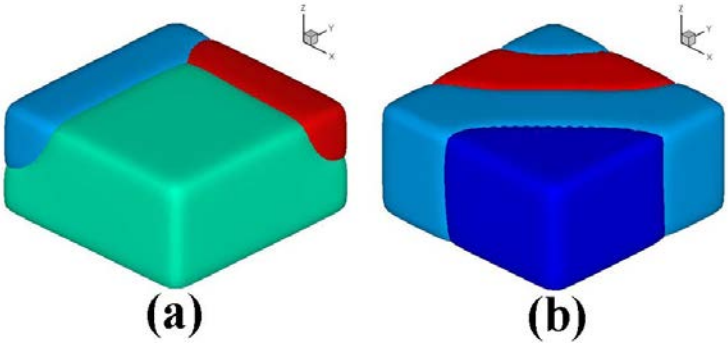

Fig. 7